

A Comparison between Liquid-Crystal Display Monitors and Cathode-Ray Tube Monitors: A Combined Assessment Study of Observer Performances by Using Storage Phosphor and Flat-Panel-Detector Radiography in Detecting Experimentally Induced Pulmonary Edema in Pigs

Sun Young Jeong¹, Myung Jin Chung², Gukmyung Choi¹, Bong Soo Kim¹, Seung Hyung Kim¹,
and Ji Kang Park¹

¹Department of Radiology, Jeju National University School of Medicine, Jeju, Korea and ²Department of Radiology, Samsung Medical Center, Sungkyunkwan University School of Medicine, Seoul, Korea

Abstract

To compare the observer performance of liquid crystal display (LCD) and cathode ray tube (CRT) monitors in detecting experimentally induced pulmonary edema in pigs by using soft-copy images of amorphous selenium-based flat-panel-detector radiography (DR) and storage phosphor computed radiography (CR). Oleic acid was injected intra-atrially into three pigs (weight, 20–25kg) at doses of 0.04, 0.05, and 0.06 ml/kg to induce pulmonary edema. Each set of CR, DR, and thin-section CT scans were obtained every 20–30 minutes from three pigs over 4–6 hours. Thus, 37 sets (10 sets from pig-1, 11 sets from pig-2, and 16 sets from pig-3) of radiographs were obtained. Images were masked for identity, randomly sorted, and displayed on both five mega pixel (2048 x 2560 x 8 bits) LCD and CRT monitors. Eight radiologists rated each image for the presence of ill defined diffuse opacities and reticular-linear opacities in both lungs by using continuous rating scale of 0–100. A total of 4736 (37 sets x 2 detector system x 2 fields x 2 lesion types x 8 observers x 2 monitor systems) observations were analyzed in terms of receiver operating characteristics. Average observer performance in detecting ill defined diffuse opacities, LCD and CRT monitors were not different significantly in both DR and CR images. Average performance in detecting reticular-linear opacities was significantly better with LCD than CRT. These differences were significant in evaluating DR images (AUC=0.852±0.038 on LCD; AUC=0.785±0.070 on CRT) but not significant in evaluating CR images (AUC=0.795±0.060 on LCD; AUC=0.745±0.070 on CRT). System on both LCD and CRT monitors ($p=0.042$ on LCD; $p=0.044$ on CRT). Moreover, with DR system, observer performance was better with LCD monitor than with CRT monitor ($p=0.013$), whereas with CR system, observer performance was not different significantly on both monitors ($p=0.118$). Overall the five-mega pixel LCD monitor was equal or superior to CRT monitor of the same pixel size in detecting experimentally induced pulmonary edema. Moreover, the LCD monitor appears to be more optimized for detecting pulmonary reticular-linear opacity, when interfaced with DR system rather than with CR system. (J Med Life Sci 2009;6:351–358)

Key Words : LCD · CRT · DR · CR · Pulmonary edema

Introduction

Over the past decade, picture archiving and communication system (PACS) have prevailed in many hospitals for its advantages, such as rapid accessibility, simultaneous image display at remote sites, reduced film or processing costs,

and easier archiving and networking of images^{1–5}. This system requires the complete digitalization of conventional screen-film projection radiography and the monitors in substitute for light boxes.

In this regard, some comparative studies between digital radiographic (DR) and computed radiographic (CR) images as the means of image acquisition have been often reported out^{6–7}. Several comparative studies between liquid crystal display (LCD) and cathode ray tube (CRT) monitors as methods of image display also have been conducted^{8–10}. However, it has not been confirmed yet the optimization of a system combination: DR and CR systems on LCD and CRT

Address for correspondence : Myung Jin Chung, MD
Department of Radiology Samsung Medical Center, Sungkyunkwan University School of Medicine 50, Ilwon-Dong, Kangnam-Ku, Seoul 135-710, Korea
E-mail : mjchung@skku.edu

monitors.

The aim of this study was to compare observer performance in detecting experimentally induced pulmonary edema in pigs via LCD and CRT monitors interfaced to DR (amorphous selenium-based flat-panel) and CR (storage phosphor) systems.

Materials and Methods

Selection of Experimental animal

The pig was used as an animal model to simulate patients with pulmonary opacities, because the pig has well-developed interlobular septa and anatomic structures that are similar to human lungs and because pigs are relatively easy to handle^{5, 11}. Three Yorkshire pigs (age, 11–13 weeks; weight, 20–25kg) were used after approval was obtained from the hospital research review board.

Animal Experimentation

Anesthesia was induced with intramuscular injection of a mixture of 7mg per kilogram of body weight of ketamine hydrochloride (Ketara; Yuhan Yanghang, Seoul, South Korea) and 2.3 mg/kg of xylazine hydrochloride (Rompun; Bayer Korea, Seoul, South Korea) and was maintained with the intravenous injection of 1.3 mg/kg of zolazepam hydrochloride (Zoletil; Virbac, Carros, France). Pigs were not intubated. A 5-Fr catheter was introduced through the right external jugular vein for the intra-atrial injection of oleic acid to induce permeability pulmonary edema. Prior to the injection of the oleic acid, baseline computed radiographic, selenium-based digital radiographic, and thin-section computed tomographic (CT) scans were obtained.

Permeability edema was induced with the intra-atrial injection of commercially available oleic acid (C18H34O2; Sigma, Steinheim, Germany) through the external jugular catheter (at doses of 0.04, 0.05, and 0.06 mL/kg as a bolus or as subdivided injections). Immediately after the injection of oleic acid, computed radiographic, selenium-based digital radiographic, and thin-section computed tomographic (CT) scans were obtained. The imaging studies were performed rapidly to minimize time delays. The interval between computed radiography and selenium-based digital radiography was as short as 1 minute because the two radiographic units were in the same room. Immediately after computed radiography and selenium-based digital radiography, the pigs were rapidly moved into the nearby CT room for CT scanning. The study sequence of computed

radiography, selenium-based digital radiography, or thin-section CT was randomly selected to avoid bias. In total, each set of computed radiographic, selenium-based digital radiographic, and thin-section CT scans were obtained in 10 minutes. Subsequently, a set of computed radiographic, selenium-based digital radiographic, and thin-section CT scans were obtained every 20–30 minutes over 4–6 hours. A total of 37 sets of images were obtained in three pigs (10, 11, 16 sets of images per pig). Each set of images included one computed radiographic image, one digital radiographic image, and one thin-section CT scan obtained during each session.

Computed Radiography and Digital Radiography

Posteroanterior chest radiographs were obtained with computed radiographic and selenium-based digital radiographic systems that were located in the same room. Two Bucky stands were set up at the opposite sides of the same room for each detector system. Computed radiographic images were obtained with an imaging unit (FCR-9000; Fuji, Tokyo, Japan). A 35 x 43-cm imaging plate (ST-V; Fuji) with a matrix of 1,760 x 2,140 x 10 bit and a pixel size of 0.2 mm was used. The selenium-based digital radiographic images were obtained by using a unit (DirectRay; Direct Radiography, Newark, Del) with a 35 x 43-cm solid-state detector with a matrix of 2,560 x 3,072 x 12 bit and a pixel size of 0.139 mm. Radiography was performed in each pig with the selenium-based digital radiographic system and then immediately after with the computed radiographic system (or vice versa).

The radiographs were produced by using the same tube and generator and at the same exposure settings, which were 80 kVp and 250 mA, with an exposure time of 50 msec and a 180-cm focus-detector distance. Both imaging systems included a moving 10:1 antiscatter grid (103 lines per inch). The x-ray beam was collimated onto the pig's chest. Immediately after the radiographs were obtained, a thin-section CT scan of the chest was obtained, or vice versa. The same technique and setting that were used to obtain the baseline thin-section CT scan were used to obtain the radiographs.

Thin-Section CT Scanning

Thin-section CT scans were obtained with a scanner (Somatom Plus 4; Siemens, Erlangen, Germany) with a field of view of 20–22 cm, a 512 x 512 matrix, an exposure of 140 kVp and 170 mA, and a 0.75-second scanning time.

Pigs were scanned in the prone position from the thoracic inlet to the level of the diaphragm with a 10-mm interval and a 1-mm section thickness. After scanning, the images were reconstructed by using a high-spatial-frequency algorithm.

Image Acquisition and Display

Digital data were saved as a Digital Imaging and Communications in Medicine (DICOM) format and then distributed to display workstations. The size of each DICOM file of the computed radiographic and selenium-based digital radiographic images was 7.18 and 15.0 Mbytes, respectively. Images were downloaded onto the local hard disk drive of the display workstation and displayed with DICOM viewer (Pi View; Infinit Technology, Seoul, Korea). Both 21-inch CRT and LCD monitors were calibrated to similar specifications: the CRT monitor (SMM21200P, Siemens AG, Germany), with 2,048 x 2,560 x 8-bit pixels, operated at 71Hz refreshing rate in an interlaced mode and at a brightness level of 450 cd/m², and LCD monitor (ME511/C; Totoku, UEDA, Nagano, Japan), with 2,048 x 2,560 x 10-bit pixels, operated at 60Hz refreshing rate and at a brightness level of 450 cd/m². The images interpreted in a darkened room. About 10% of the display area was allocated for the title and menu bars, and the remaining display area (2,048 x 2,300 pixels) was large for the computed radiographic data and slightly small for the selenium-based digital radiographic data. Therefore, selenium-based digital radiographic images were displayed as its original resolution and computed radiographic images were enlarged by 50% by using pixel replication to fit the remaining monitor display area. The soft-copy images were displayed without unsharp masking. Only the window widths and the image levels were optimized automatically with a customized program, which produced the same density for the computed radiographic and selenium-based digital radiographic images. No other image postprocessing was performed. Observers were allowed to adjust the brightness and contrast of the images. For this study, pig identification was obscured on all images and replaced by a sequence number. Computed radiographic and selenium-based digital radiographic images were displayed in a random manner.

Image Interpretation

Eight radiologists served as observers for the study; four of them were board-certified radiologist, and the others were residents in department of radiology. All they were

accustomed to a PACS viewer because they used it in daily practice. They evaluated the images independently. The images were masked for identity and assigned randomly to prevent selection bias. Observers divided the lesion types into two groups (ill defined diffuse opacities and reticular-linear opacities) and a continuous rating scale of 1 - 99 was used to represent each observer's confidence level regarding the presence or absence of diffuse hazy opacity and reticular-linear opacity. Half of the observers had their rating session with the CRT monitor first, the other half with the LCD monitor first. Each reading session was separated by at least 1 week to diminish learning effect.

All 37 thin-section CT scans of the chest were evaluated by two board-certified chest radiologists, and decisions about the presence of pulmonary edema were reached with a consensus.

Statistical Analysis

A total of 4736 observations (37 sets x 2 detector system: CR and DR x 2 fields: right and left lung field x 2 lesion types: ill defined diffuse opacities and reticular-linear opacities x 8 observers x 2 monitor systems: LCD and CRT) were evaluated. Observer performance in detecting experimentally induced pulmonary edema in pigs by observing LCD and CRT monitors interfaced to DR and CR systems was tested by using receiver operating characteristic (ROC) analysis of individual reader data. All statistical analyses were performed by using SPSS for Window v12.0 (SPSS industry, Chicago, IL). Detection accuracy was measured according to the area under the ROC curve, or AUC value. Differences between the monitor systems combined with the digital detector systems and lesion types were compared using the paired t test. The statistical significance of the results was reported as 95% CIs for mean differences in AUC values for observer performance¹²⁾. Mean differences were regarded as statistically significant at the 5% level when the corresponding CI did not encompass zero¹²⁾.

Results

Mean AUC values are given in Table 1 to illustrate the observer performance for the detection of experimentally induced pulmonary edema in pigs. The 95% CIs for the differences between the monitor systems and the detector systems are also provided (Table 2, 3).

This is a total combination comparative study including

comparison of DR vs CR systems, LCD vs CRT monitors, and lesion types (alveolar consolidation vs interstitial density).

First, we looked at the comparison studies of LCD and CRT performance. In all the four combination (diffuse hazy opacity on CR, reticular-linear opacity on CR, diffuse hazy opacity on DR, and reticular-linear opacity on DR), LCD performed better than CRT. However, only in the combination of DR and detecting reticular-linear opacity showed a statistically significant difference ($p=0.013$) (Table 2).

Comparing CR and DR, there is no significant difference between CR and DR in evaluating diffuse hazy opacity, but DR was better significantly than CR in evaluating reticular-linear opacity with both CRT and LCD monitor combinations ($p=0.044$ on CRT, $p=0.042$ on LCD) (Table 3).

Comparing lesion types, CR and LCD combination showed the highest AUC average score in evaluating diffuse hazy opacity, but there is no significant difference in comparing the rest three combinations. In evaluating reticular-linear opacity, it was proved that DR and LCD combination

performed the best with statistically significant difference compared to the rest three combinations (Table 4).

ROC curves from the different combination of monitors and lesion types for each eight radiologist are shown in Figure 1.

Discussion

Many investigators have reported equivalent or superior performance with the use of DR system compared to CR system in detecting pulmonary lesions^{5, 6}. Thus flat-panel digital radiographic system has already been widely used in daily radiology practice of many institutes as well as storage-phosphor computed radiographic system. The current study confirmed significantly better performance with the use of DR system than that of CR system in detecting reticular and linear opacities, although the DR and CR system's performance remained constant in detecting diffuse hazy opacities. These results are attributed to the superiority

Table 1. Mean values of area under curve (AUC) in receiver operating characteristic analysis in detecting experimentally induced pulmonary edema in pigs; comparison of four combinations in LCD and CRT monitors interfaced to DR and CR systems

	Diffuse hazy opacity				Reticular-linear opacity			
	CR-CRT	DR-CRT	CR-LCD	DR-LCD	CR-CRT	DR-CRT	CR-LCD	DR-LCD
Mean	0.753	0.755	0.779	0.758	0.745	0.785	0.795	0.852
N	8	8	8	8	8	8	8	8
SD	0.052	0.091	0.054	0.082	0.070	0.070	0.060	0.038
SE	0.019	0.032	0.019	0.029	0.025	0.025	0.021	0.013

Abbreviations. CRT; cathode ray tube, LCD; liquid crystal display, CR; computed radiography, DR; digital radiography, SD; standard deviation, SE; standard error

Table 2. Comparison between LCD and CRT monitors by the differences of AUC values for detecting two lesion types.

	AUC(CRT) - AUC(LCD)			
	Diffuse hazy opacity		Reticular-linear opacity	
	CR	DR	CR	DR
Mean	-0.025	-0.003	-0.051	-0.067
SD	0.082	0.066	0.081	0.058
SE	0.029	0.023	0.029	0.020
Mean 95% CI				
Lower	-0.094	-0.058	-0.118	-0.115
Upper	0.043	0.053	0.017	-0.019
t	-0.875	-0.107	-1.784	-3.283
p (2-tailed)	0.410	0.918	0.118	0.013

Abbreviations. - CRT; cathode ray tube, LCD; liquid crystal display, CR; computed radiography, DR; digital radiography. SD; standard deviation, SE; standard error, CI; confidence interval

Note. - CIs, t values, and p values were calculated by paired sample T-test.

of digital radiography compared to the computed radiography in terms of spatial resolution.

Theoretically, digital radiography, which has a matrix of 2,560 x 3,072 pixels (139 x 139 μm per pixel), can depict more fine details than can computed radiography with a matrix of 1,760 x 2,140 pixels (200 x 200 μm per pixel). Pixel size is an important parameter in digital radiography because it directly influences the spatial resolution of images, particularly in the depiction of fine detail^{5, 13}.

Another explanation for the better performance of digital radiography is related to the absence of light scattering within the detector. Even if other factors such as the matrix and pixel sizes were equal, sharper images could be

obtained with digital radiography than with screen-film radiography or computed radiography. The conversion of x-ray photons to electrical charges and electrical data is direct by means of arrays of semiconductor elements without the intervening light stage, such as in an intensifying screen or a photostimulable phosphor imaging plate. The latter are used in the screen-film system and computed radiography, respectively. In the screen-film system and computed radiography, light scattering of intermediate light fluorescence results in image blurring^{5, 6, 14}.

Another factor related to the detection of pulmonary abnormalities on chest radiographs is the image gray scale. The number of gray levels in a digital system determines

Table 3. Comparison between CR and DR systems by the differences of AUC values for detecting two lesion types

	AUC(CR) - AUC(DR)			
	Diffuse hazy opacity		Reticular-linear opacity	
	CRT	LCD	CRT	LCD
Mean	-0.002	0.021	-0.040	-0.056
SD	0.069	0.075	0.046	0.064
SE	0.025	0.027	0.016	0.023
Mean 95% CI				
Lower	-0.060	-0.042	-0.079	-0.110
Upper	0.056	0.084	-0.002	-0.003
t	-0.076	0.790	-2.456	-2.479
p (2-tailed)	0.942	0.456	0.044	0.042

Abbreviations. - CRT: cathode ray tube, LCD; liquid crystal display, CR: computed radiography, DR: digital radiography, SD: standard deviation, SE: standard error, CI: confidence interval

Note. - CIs, t values, and p values were calculated by paired sample T-test.

Table 4. Statistical analysis of the differences of best combination from others according to the lesion types

Best Combination	Diffuse hazy opacity (CR-LCD)			Reticular-linear opacity (DR-LCD)		
	vs. CR-CRT	vs. DR-CRT	vs. DR-LCD	vs. DR-CRT	vs. CR-LCD	vs. CR-CRT
Mean difference	0.025	0.024	0.021	0.067	0.056	0.107
SD	0.082	0.082	0.075	0.058	0.064	0.071
SE	0.029	0.029	0.027	0.020	0.023	0.025
Mean 95% CI						
Lower	-0.094	-0.045	-0.042	-0.115	-0.110	-0.167
Upper	0.043	0.092	0.084	-0.019	-0.003	-0.048
t	-0.875	0.812	0.790	-3.283	-2.479	-4.273
p (2-tailed)	0.410	0.443	0.456	0.013	0.042	0.004

Abbreviations. - CRT: cathode ray tube, LCD; liquid crystal display, CR: computed radiography, DR: digital radiography, SD: standard deviation, SE: standard error, CI: confidence interval

Note. - CIs, t values, and p values were calculated by paired sample T-test.

how well it reproduces subtle contrast differences. Selenium-based digital radiographic images are digitized in 12-bit gray scale (4,096 shades), whereas most of the currently used computed radiographic systems provide 10-bit images (1,024 shades). Some computed radiographic systems that can create 12-bit images are now also commercially available. Therefore, selenium-based digital radiography can, theoretically, more accurately depict the subtle variations in attenuation¹⁵. According to a study by Floyd et al¹⁶, measurement of inherent contrast sensitivity showed little difference between the flat-panel-detector and storage phosphor systems. However, because the inherent contrast of the two detectors was comparable and because the noise power spectrum of the flat-panel-detector system was far superior to that of the storage-phosphor system, one may conclude that contrast-to-noise ratio of the former should also be superior to that of the latter¹⁶.

It is established that CRT monitor can replace

conventional radiographs successfully^{4, 17}. Many authors reported that LCD and CRT monitors are comparable⁸⁻¹⁰. In our study, LCD performed better than CRT in all the four combinations (diffuse hazy opacity on CR, reticular-linear opacity on CR, diffuse hazy opacity on DR, and reticular-linear opacity on DR) although the statistically significant difference was only seen with the combination of detecting reticular-linear opacity ($p=0.013$) (Table 2) (Figure 1). We guess that Reticular-linear opacities are better delineated by sharper edges; therefore the lesion may be conspicuous in image of higher spatial resolution and less pixel blurring. We also guess that ill defined diffuse opacities are better delineated by higher contrast differences therefore the lesion may be conspicuous in image of higher gray scale. The pixel pointed on CRT monitor shows larger spot size and blurred edge than its original data because of electron beam divergence; this phenomenon is more severe at higher luminance. On the other hand, spatial characteristics of LCD

Figure 1. Receiver operating characteristic (ROC) curves according to the combination of monitor, detector and lesion type for eight observers.

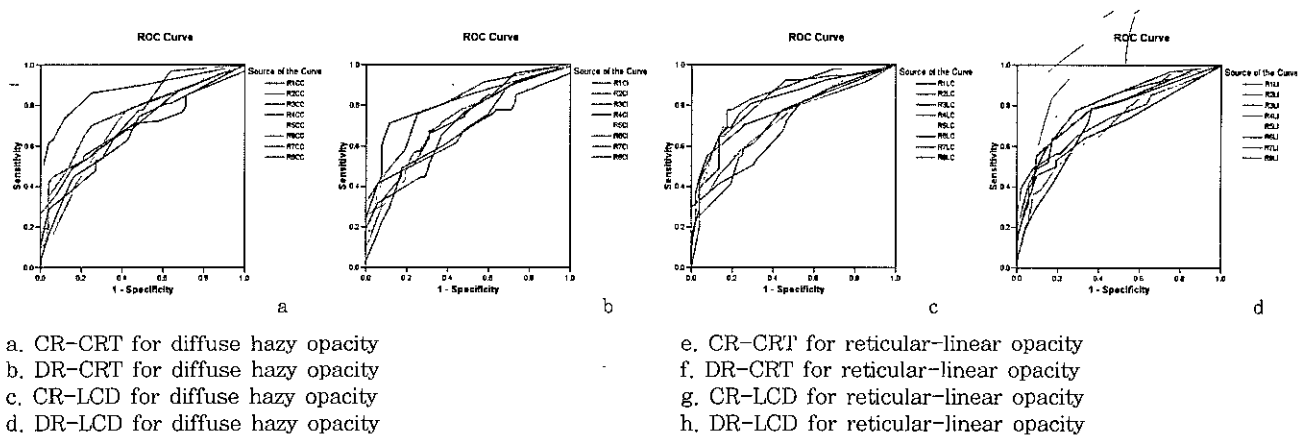
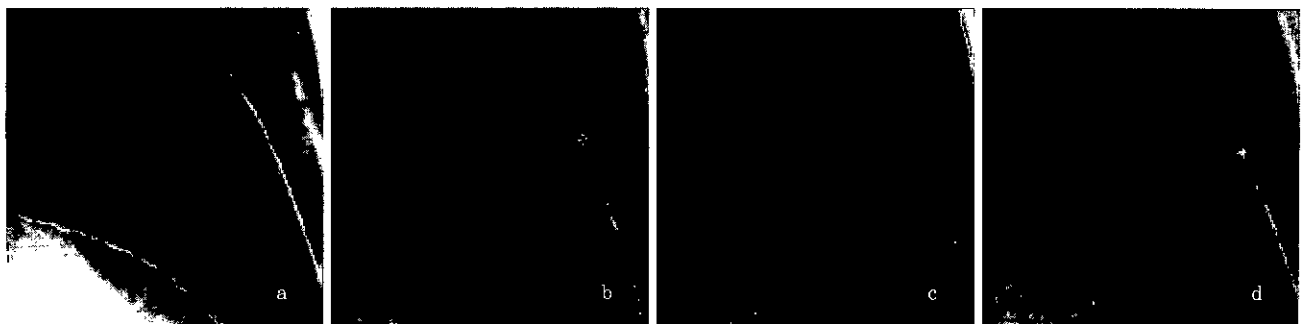


Figure 2. RMagnified photograph of four imaging system - monitor combinations. (a) Storage phosphor computed radiograph (CR) displayed on cathode ray tube (CRT) monitor. (b) Selenium-based flat panel digital radiograph (DR) displayed on CRT, (c) CR displayed on liquid crystal display (LCD) monitor, and (d) DR displayed on LCD. Subtle reticular opacities are demonstrated better on (d) than others. Tilted stripes seen on (c) and (d) are moire artifact because of the interference between the array of CCD in digital camera and the pixel lines of LCD panel.



is close to ideal response up to the Nyquist frequency associated with the display pixel size¹⁸). Thus the pixel sharpness of LCD monitor is much better than those of CRT.

CRT monitors suffer from several drawbacks. First, they are heavy and bulky, and a pair of CRT monitors needs a lot of space in the reading room. Second, CRT monitors are not completely flicker free. Third, at very high resolutions, CRT pixels often suffer a certain degree of fuzziness. Fourth, CRT monitors have a limited life span, because their maximum brightness decreases over time and pixels may be burned into the phosphor coating of the CRT. Fifth, CRT monitors usually present some degree of geometric distortion. Lastly, CRT monitors emit considerable amount of heat and electromagnetic waves. In contrast, high-resolution LCD monitors are clean, slim, energy effective, and cost effective. Display quality of LCD monitor is consistent through its whole life cycle.

As mentioned earlier, over the past years there have been many studies regarding the performance comparison on DR vs. CR, and LCD vs. CRT, and the findings are relatively consistent and stable. However, previous studies were not extensive enough to include combinations of both variables (monitor and detector system) to explore which detector system by which monitor could deliver the best image quality. The present study confirmed that spatial resolution of target image can be displayed best with the combination of LCD monitor and DR system. This study is meaningful in a sense that it confirms the existing research findings on DR vs. CR and LCD vs. CRT, but also explores the most optimized reading environment via various combination assessments.

The major limitation of our study is that the study was based on the pig's lung by injecting oleic-acid experimentally, not an actual patient's lung. Therefore, the result of this study cannot exactly represent a human patient's lesion. However, pig has relatively well-developed interlobular septa and pig's anatomic structure is similar to that of human lung^{5, 11}). Thus pig's lung can simulate many disease conditions of human lung. Another limitation of this study can be that observers were not accustomed to chest radiography of pig. Regarding this concern, we had several practice sessions with some image pictures to learn pig's chest anatomy before we actually start main study.

In conclusion, overall five-mega pixel LCD monitor was equal or superior to CRT monitor of the same pixel size in detecting experimentally induced pulmonary edema. Moreover, the LCD monitor appears to be more effective

(statistically significant) for detecting reticular-linear densities when interfaced with DR system rather than with CR system.

References

- 1) Razavi M, Sayre JW, Taira RK, et al. Receiver-operating-characteristic study of chest radiographs in children: digital hard-copy film vs 2K x 2K soft-copy images. *AJR Am J Roentgenol* 1992; 158:443-448.
- 2) Hayrapetian A, Aberle DR, Huang HK, et al. Comparison of 2048-line digital display formats and conventional radiographs: an ROC study. *AJR Am J Roentgenol* 1989; 152:1113-1118.
- 3) Slasky BS, Gur D, Good WF, et al. Receiver operating characteristic analysis of chest image interpretation with conventional, laser-printed, and high-resolution workstation images. *Radiology* 1990; 174:775-780.
- 4) Ishigaki T, Endo T, Ikeda M, et al. Subtle pulmonary disease: detection with computed radiography versus conventional chest radiography. *Radiology* 1996; 201:51-60.
- 5) Kim TS, Im JG, Goo JM, et al. Detection of pulmonary edema in pigs: storage phosphor versus amorphous selenium-based flat-panel-detector radiography. *Radiology* 2002; 223:695-701.
- 6) Goo JM, Im JG, Lee HJ, et al. Detection of simulated chest lesions by using soft-copy reading: comparison of an amorphous silicon flat-panel-detector system and a storage-phosphor system. *Radiology* 2002; 224:242-246.
- 7) Garmer M, Hennigs SP, Jager HJ, et al. Digital radiography versus conventional radiography in chest imaging: diagnostic performance of a large-area silicon flat-panel detector in a clinical CT-controlled study. *AJR Am J Roentgenol* 2000; 174:75-80.
- 8) Kotter E, Bley TA, Saueressig U, et al. Comparison of the detectability of high- and low-contrast details on a TFT screen and a CRT screen designed for radiologic diagnosis. *Invest Radiol* 2003; 38:719-724.
- 9) Hwang SA, Seo JB, Choi BK, et al. Liquid-crystal display monitors and cathode-ray tube monitors: a comparison of observer performance in the detection of small solitary pulmonary nodules. *Korean J Radiol* 2003; 4:153-156.
- 10) Partan G, Mayrhofer R, Urban M, Wassipaul M, Pichler L, Hruby W. Diagnostic performance of liquid crystal and cathode-ray-tube monitors in brain computed tomography. *Eur Radiol* 2003; 13:2397-2401.
- 11) Murata K, Herman PG, Khan A, Todo G, Pipman Y,

- Luber JM. Intralobular distribution of oleic acid-induced pulmonary edema in the pig. Evaluation by high-resolution CT. *Invest Radiol* 1989; 24:647-653.
- 12) Bulpitt CJ. Confidence intervals. *Lancet* 1987; 1:494-497.
- 13) Chotas HG, Dobbins JT, 3rd, Ravin CE. Principles of digital radiography with large-area, electronically readable detectors: a review of the basics. *Radiology* 1999;210:595-599.
- 14) Rowlands JA, Zhao W, Blevis IM, Waechter DF, Huang Z. Flat-panel digital radiology with amorphous selenium and active-matrix readout. *Radiographics* 1997; 17:753-760.
- 15) MacMahon H, Vyborny C. Technical advances in chest radiography. *AJR Am J Roentgenol* 1994; 163:1049-1059.
- 16) Floyd CE, Jr., Warp RJ, Dobbins JT, 3rd, et al. Imaging characteristics of an amorphous silicon flat-panel detector for digital chest radiography. *Radiology* 2001; 218:683-688.
- 17) Thaete FL, Fuhrman CR, Oliver JH, et al. Digital radiography and conventional imaging of the chest: a comparison of observer performance. *AJR Am J Roentgenol* 1994; 162:575-581.
- 18) Blume HR, Steven PM, Cobb ME, et al. Characterization of high-resolution liquid crystal displays for medical images. *Proc SPIE* 2002; 4323-07:271-292.